Colloid Polym Sci (2005) 283: 1050–1055
DOI 10.1007/s00396-004-1255-4

ORIGINAL CONTRIBUTIONS

Preparation of ultrathin membranes by layer-by-layer deposition of layered double hydroxide (LDH) and polystyrene sulfonate (PSS)

V. Hornok
A. Erdőhelyi
I. Dékány

Received: 30 August 2004
Accepted: 18 October 2004

V. Hornok · I. Dékány (✉)
Department of Colloid Chemistry,
Nanostructured Materials Research Group
of the Hungarian Acadamy of Sciences,
University of Szeged,
Aradi Vértanúk tere 1,
6720 Szeged, Hungary
E-mail: i.dekany@chem.u-szeged.hu

A. Erdőhelyi
Department of Solid State and
Radiochemistry, University of Szeged,
Aradi Vértanúk tere 1,
6720 Szeged, Hungary

Abstract Nanofilms were prepared by consecutively alternating adsorption of Mg–Al (2:1) layered double hydroxide (LDH) and polysodium 4-styrenesulfonate (PSS). The charge density of oppositely charged materials strongly affect film properties like thickness and ordering. The specific charge of the colloid particles (LDH) and macromolecules was determined with the particle charge detector. The sequential build-up of the thin films was followed by spectrophotometry and X-ray diffraction. The surface morphology of the multilayers was characterized by atomic force microscopy. The influence of the charge density of the applied materials and of the mass ratio of LDH/PSS on the film thickness were studied.

Keywords Layered double hydroxides · Membranes · Multilayers

Introduction

Application of multilayered nanofilms in membrane technology requires tailored film properties with a well-known structure. The size of discontinuities in nanostructured materials makes membranes able to separate different particles by filtration so that these materials gain widespread application in nanotechnology for separating fluids and gases. The micro- and nanopore containing materials like zeolites and activated carbon are well known in the separation of C_4–C_6 hydrocarbons or CO_2 from CH_4, hydrocarbons from natural gas or CO_2 from N_2 [1–6]. Applied nanostructured materials in our present knowledge are chemically homogeneous like silicates, carbons, polymers etc. Polymer/phyllosilicate multilayer films were already prepared by layer-by-layer deposition [7–17]. The structure is stabilised by electrostatic forces between the negatively charged silicates like montmorillonite and the positively charged cationic polyelectrolyte. The adsorbed polymer layers on any planar surface (glass or polymer) order the nanothin silicate lamellae [7, 8].

Layered doubled hydroxides are natural or synthetic materials composed of positively charged octahedral sheets separated by exchangeable anions (Cl^-, NO_3^-, CO_3^{2-}, SO_4^{2-}) and water molecules. The crystallographic, physical and chemical properties, particle size and specific area depend on the way of preparation and the composition of the starting mixtures. The size of anions determines the layer distance [18]. The general formula of LDHs are: $[M_{1-x}^{2+}\ M_x^{3+}\ (OH)_2]\ (A^{n-})_{x/n}\cdot yH_2O$, where M^{2+} can be Mg^{2+}, Fe^{2+}, Co^{2+}, Ni^{2+}, Zn^{2+} and M^{3+} may be Al^{3+}, Cr^{3+}, Fe^{3+}, Co^{3+} [19, 20]. Several industrial applications are known. LDHs

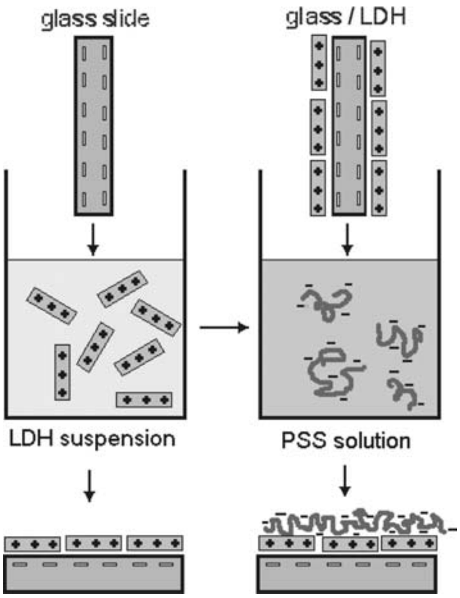

Fig. 1 LDH/PSS nanofilm preparation by layer-by-layer immersion technique

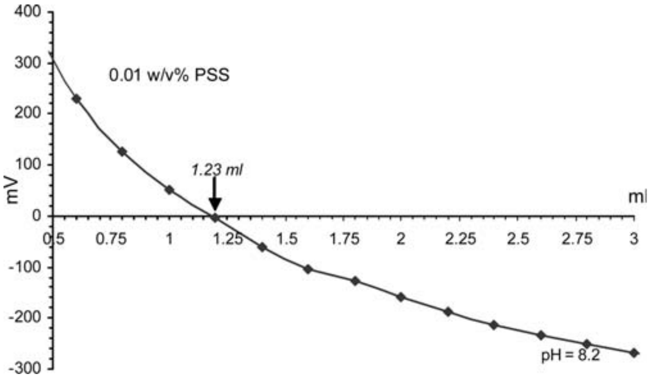

Fig. 2 Charge titration (PCD) of 1 w/v% Mg-Al LDH suspension by 0.01 w/v% PSS solution

are used in air and water purification, as catalysts in production of intermediates and fine chemicals [21, 22], in various hydrogenating processings. Surprising but promising experiments were performed in applying LDHs in photochemistry, medicine and enviromental chemistry [23]. LDHs polyanions were used to prepare membranes. Ultrathin membranes form in the colloid suspension and in aqueous polymer solutions by applying the immersion technique in which the layers of positively charged LDH and negatively charged polymer layers alternate. Inorganic colloid particles can also be used to form membranes of LDHs with phyllosilicates or negatively charged particles. Heterocoagulation occurs between the two inorganic oppositely charged particles. The membranes are stabilized by electrostatic

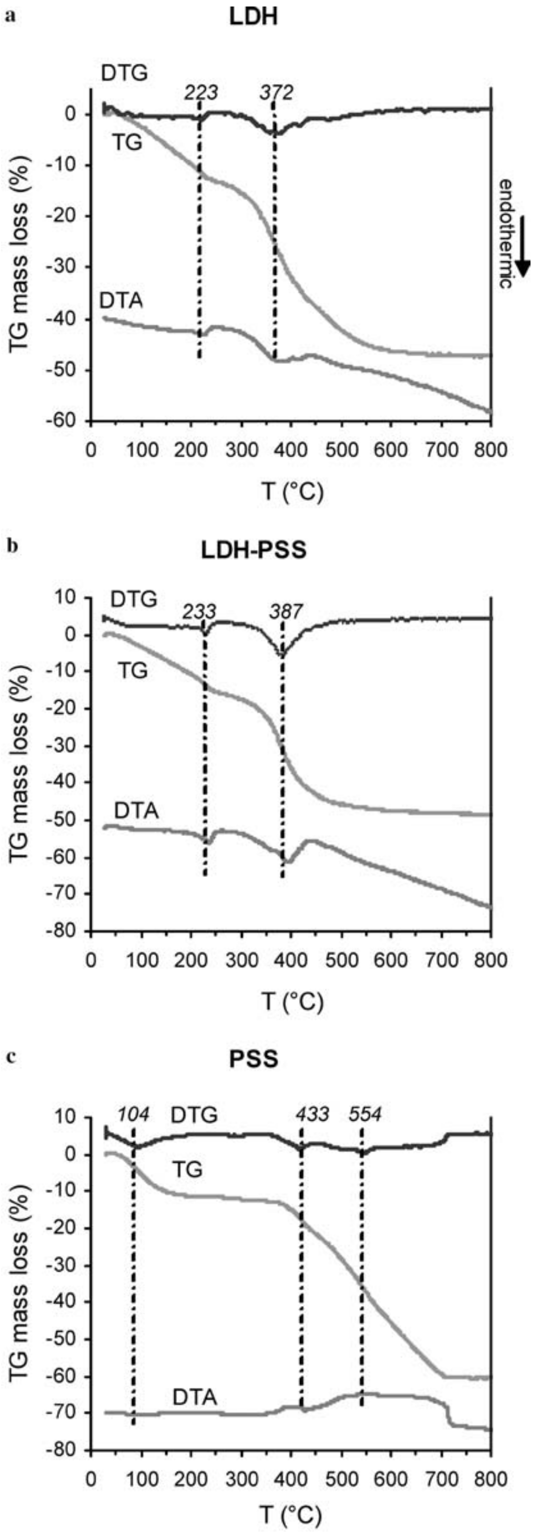

Fig. 3 Thermogravimetric (TG), differential thermogravimetric (DTG) and differential termoanalytic (DTA) curves of **a** LDH; **b** LDH/PSS composite; **c** PSS

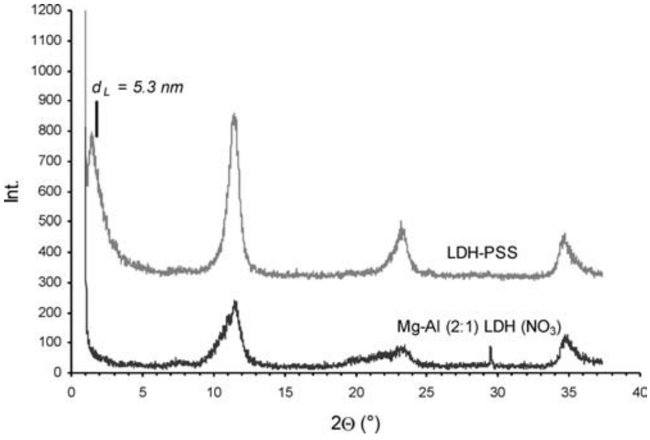

Fig. 4 XRD-patterns of LDH powder and LDH/PSS composite

forces and stable layers are formed in the ca. 10–100 nm size range.

Materials and methods

A hydrotalcit-type LDH Mg–Al (2:1) was prepared from aluminium nitrate nonahydrate ($Al(NO_3)_3 \cdot 9H_2O$) and magnesium nitrate hexahydrate ($Mg(NO_3)_2 \cdot 6H_2O$). The two compounds were dissolved in boiled-off distilled water before the NaOH containing $NaNO_3$ solution was added dropwise and was stirred for 5 h in N_2 atmosphere at 60 °C and then subsequently at ambient temperature (hold in N_2): The precipitated LDH was washed with water and dried at 65 °C. The powdered sample obtained was characterized by X-ray powder diffraction and thermoanalytic measurements.

The sodium salt of polystyrene sulfonate (PSS, Aldrich) was applied as the negative component of film preparation. 0.5 and 1 w/v% of LDH suspensions and 0.25, 0.5 and 1 w/v% of polymer solution were used. The nanofilms were prepared on Menzel Superfrost glass (Fischer Sci. Co.) by layer-by-layer deposition (Fig.1).

The charge of LDH and PSS was measured by the particle charge detector (PCD2, Mütek Analytic GmbH, Germany) [24, 25]. For the PCD titration the cationic sufactant hexadecylpyridinium chloride (HDPCl) was used to determine the specific charge of the negatively charged macromolecule. The so-called charge equivalent points belonging to zero potential was used to calculate the specific charge of PSS, 4.1 meq/g. The negatively charged PSS was mixed with the LDH suspension in different volumes and potential values were detected after 20 min equlibrium time. A volume of 1.23 cm^3 0.01 w/v% PSS solution was sufficient to neutralise 10 cm^3 1 w/v% LDH suspension (Fig. 2).

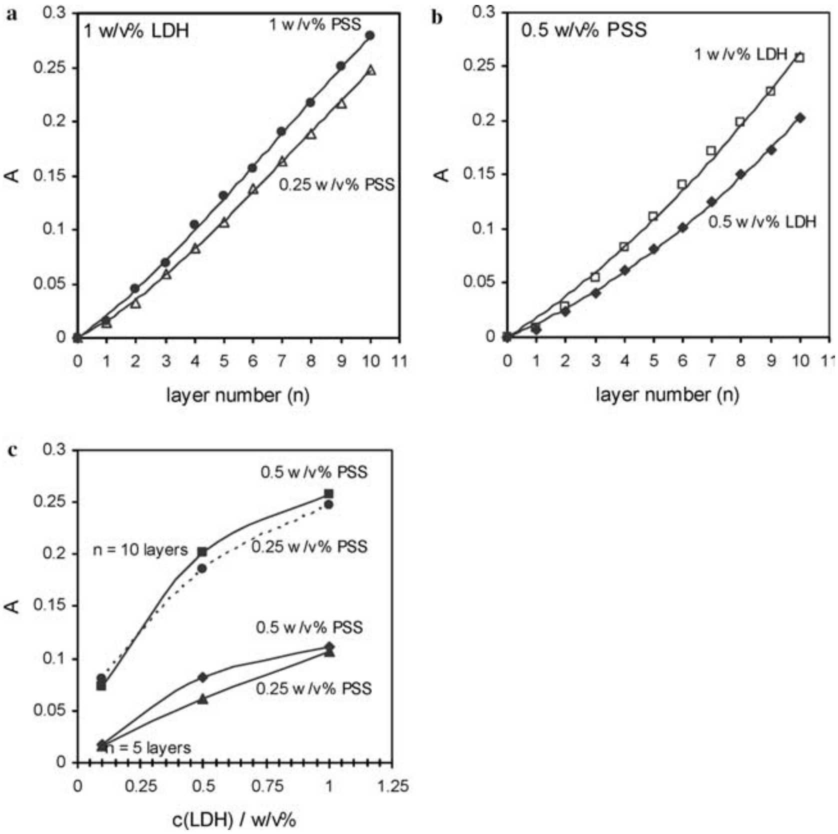

Fig. 5 Absorbency measurements of LDH/PSS films. **a** deposition of 1 w/v% LDH suspension with 1 w/v% and 0.5 w/v% PSS solution; **b** deposition of 0.5 w/v% LDH suspension with 1 w/v% and 0.5 w/v% PSS solution; **c** absorbance as a function of LDH concentration at $n = 5$ and 10 layers

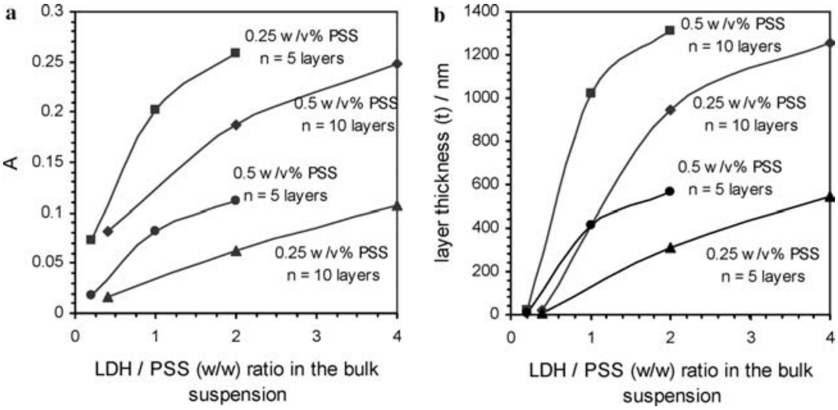

Fig. 6 Absorbance measurements of LDH/PSS films. **a** influence of the LDH/PSS ratio on light absorption properties of the films at different *n* and PSS concentrations; **b** the influence of the LDH/PSS ratio on the thickness at different *n* and PSS concentrations

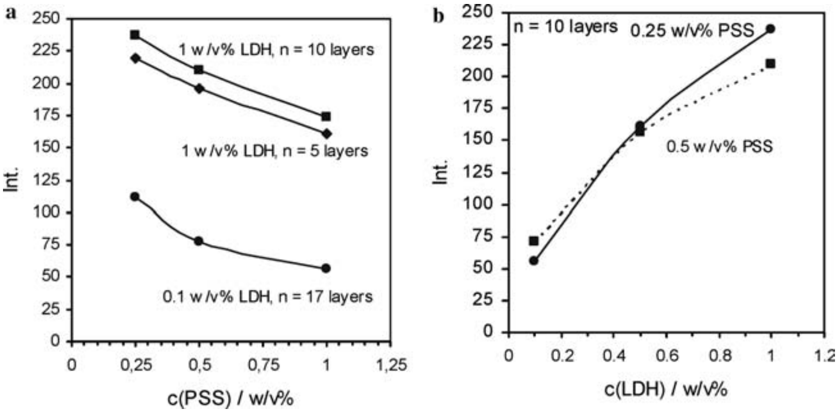

Fig. 7 Intensity of the basal reflection **a** versus PSS concentration at constant *n*; **b** versus LDH concentration at constant *n*

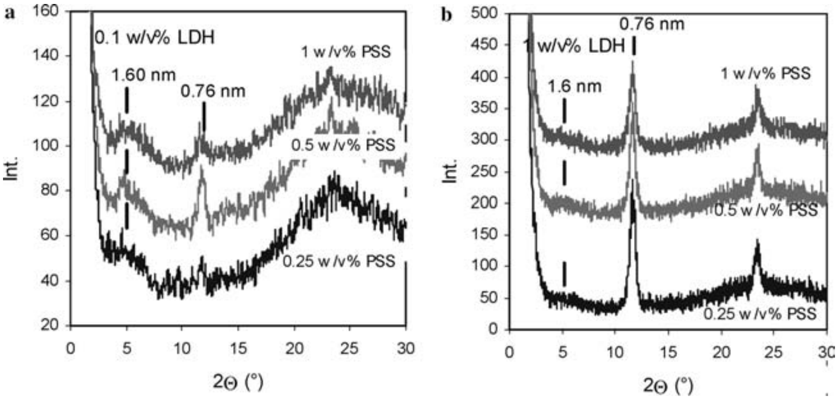

Fig. 8 XRD patterns of LDH/PSS nanofilms. **a** deposition from 0.1 w/v% of LDH suspension at different PSS concentrations at $n=17$; **b** deposition from 1 w/v% LDH suspension at different PSS concentrations at $n=10$

Light absorbance of the films was measured with the Uvikon 930 UV-Vis two-way spectrophotometer. We recorded the absorbency after deposition of every layer. The results were corrected by considering the absorbance of the glass silde. X-ray diffraction (XRD) measurements were performed in a goniometer fitted to a Philips PW 1820 generator (CuK$_\alpha$, 40 kV, 30 mA; Ni grids as filter). The basal spacing was derived from the basal reflections (00l).

The morphology of the films was observed by the AFM Nanoscope III (Digital Instruments, USA) piezo scanner with scanning capability of 12.5 μm in *x* and *y* direction and 3 μm in *z* direction, tapping-type tip of silicon (Veeco Nanoprobe Tips RTESP model, 125 μm length, 300 kHz).

Thermoanalytic measurements were performed by the Derivatograph Q-1500-D (MOM, Hungary). The powder samples were heated from room temperature to

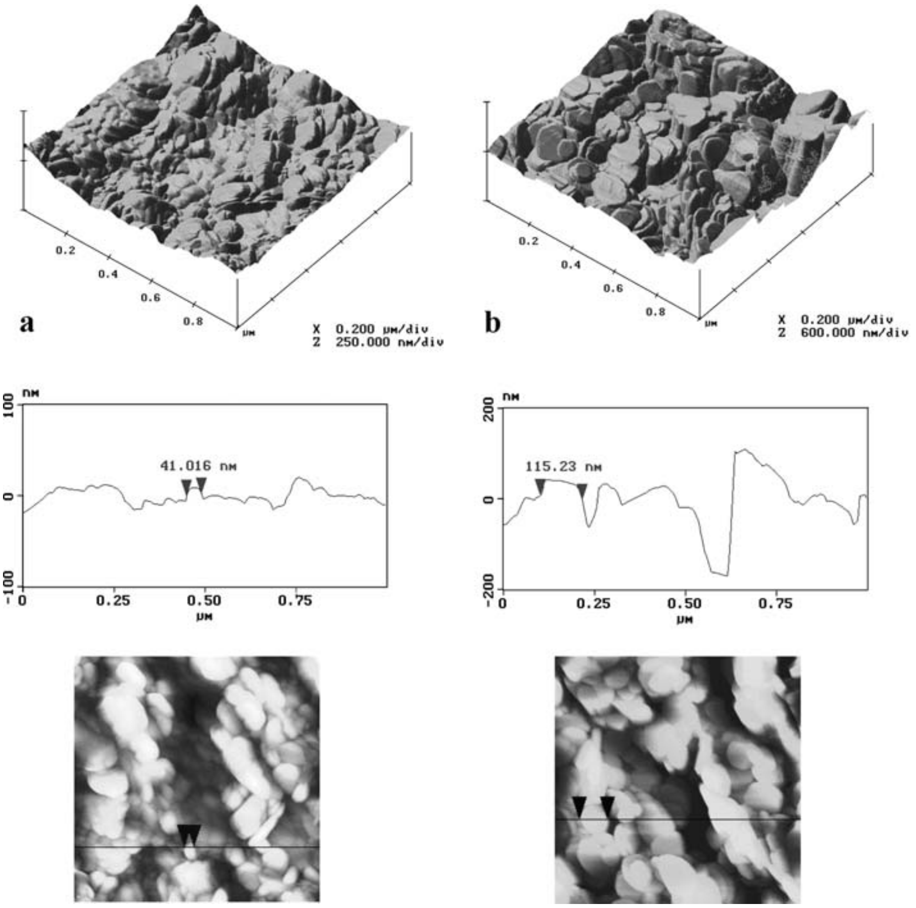

Fig. 9 AFM images of LDH/PSS multilayers after deposition on the glass surface. **a** 0.1 w/v% LDH suspension and 0.25 w/v% PSS solution at $n = 17$ (PSS/LDH = 2.5); **b** 1 w/v% LDH and 0.25 w/v% of PSS solution at $n = 10$ (PSS/LDH = 0.25)

1,000 °C with 5 °C/min, mass-stable Al_2O_3 was used as the reference.

Prior to film preparation the glass slides were cleaned in chromic acid for several hours to remove contaminations, then carefully washed with distilled water and dried. The (negative) glass slides were immersed in the LDH-suspension for 10 min followed by rinsing with distilled water to remove the excess of suspension. An ultrathin LDH monolayer forms on the surface (Fig. 1). The positively charged LDH-film adsorbed the polyanions when immersed into the polymer solution so that a one-layer LDH/PSS hybrid film formed on the glass surface. The immersion period was 10 min followed by half a minute rinsing with distilled water and drying with N_2.

Results and discussion

In order to gain information about interaction between PSS and the LDH bulk-phase charge equivalent amounts of PSS were added to LDH suspensions. After the coagulation, the precipitates were filtered, dried and characterized by XRD and thermogravimetric measurements (Fig. 3). TG and DTG curves of LDH indicates two endothermic reactions at 223–372 °C: dehydration of the interlayer water at 200–223 °C; nitrate decomposition, escape of nitrogen oxides and further dehydroxylation at 372 °C. For LDH/PSS the position of the two peaks is shifted to somewhat higher temperatures (Fig. 3b). The loss of water in pure PSS takes place at about 100 °C and further dehydration of the structural OH-groups occurs at ≥433 °C (Fig. 3c). The prolonged exothermic peak indicates the combustion of carbon at 554 °C.

Results of XRD measurements of LDH and LDH/PSS are represented in Fig. 4. The Bragg reflection at $d = 5.3$ nm shows the distance of the LDH particles in the composite.

LDH/PSS films were produced from a suspension of 0.1 w/v% LDH with PSS concentrations of 0.25 w/v%, 0.5 w/v% and 1 w/v%; then more concentrated LDH suspensions of 0.5 and 1 w/v% were applied. Results of spectrophotometric measurements at $\lambda = 400$ nm are shown in Fig. 5. Light absorbance of the films increases linearly with the number n of layers when $n > 5$. The absorption is also proportional to the layer thickness ($n = 10$: ten layers PSS and ten LDH layers). The effect of LDH concentration on the light absorbance at constant polymer concentration is seen in Fig. 5c. Light absorption barely changes with the amount of polymer while the LDH concentration significantly influences this property. The influence of the PSS/LDH mass ratio in the bulk liquid phase is shown in Fig. 6. The higher the LDH/PSS ratio, the thicker the films and the slope decreases. The reflections characteristic of double hydroxide at $2\Theta = 11.7°$ and 23.4° and of the LDH intercalation compound at 5.5° appear in every XRD pattern. The intensity of the Bragg reflections characteristic of LDH decreases with increasing concentration of the anionic polymer, which indicates the insertation of higher amounts of polymer in the film (Fig. 7a). The intensity of Bragg reflection also significantly depends on the suspension concentration (for $n = 10$ see Fig. 7b). Films made from 0.5 w/v% and 1 w/v% LDH suspensions and containing five layers of LDH/PSS indicate a basal spacing of 0.76 and 0.38 nm. The experiments demonstrate that the diluted PSS-solution is sufficient to produce higher amounts of LDH in the multilayer film (Fig. 8). The higher the concentration of the polymer, the lower the XRD peak intensity; thus, higher amounts of PSS reduce the LDH binding in the film.

The AFM images of films prepared from 0.1 w/v% and 1 w/v% LDH suspensions and 0.25 w/v% of PSS are seen in Fig. 9a and 9b. Both images show 1 μm×1 μm areas and the height is charted in the 250 and 600 nm range. The difference between the two images is evident: less-ordered superpositioned lamellae by appling 0.1 w/v% of LDH and well-ordered disc-like structures at 1 w/v% LDH. The more highly ordered structure (Fig. 9b) confirms the results of XRD measurements.

To determine the film thickness, the deposited amount of LDH was calculated from the absorbance values by using a calibration curve (absorbency vs. LDH amount). From the mass of films and an assumed density ($\delta_{LDH/PSS} = 1.42$ g/cm^3) the film area and thickness were determined. The thickness changed between 1,020 nm and 1,300 nm, in accordance with the results of other measurements.

Conclusions

Nanofilms of LDH/PSS were prepared and characterised by light absorbency, XRD and AFM measurements. At too high PSS/LDH mass ratio thinner films were formed because the polymer forces the suspension down from the surface during immersion. Well-ordered films were obtained from diluted PSS solutions. Changing the polymer concentration at constant LDH concentration causes only weak difference while the LDH concentration is more important. As the charge of PSS is much higher than that of the LDH lamellae, an increase in PSS concentration does not lead to the insertion of a larger number of LDH layers.

Acknowledgements The authors wish to convey their thanks for the financial support of the Hungarian Scientific Fund (OTKA) T 043430 and for the Ministry of Education NKFP 03/047/2001.

References

1. Kalipcilar H, Gade SK, Noble RD, Falconer JL (2002) J Membr Sci 210:113–127
2. Tomita T, Nakayama K, Sakai H (2004) Micropor Mesopor Mater 68:70–75
3. Tuan VA, Li S, Falconer JL, Noble RD (2002) J Membr Sci 196:111–123
4. Arruebo M, Coronas J, Menéndez M, Santamaría J (2001) Sep Pur Tech 25:275–286
5. Kusakabe K, Kuroda T, Morooka S (1998) J Membr Sci 148:13–23
6. Menard D, Py X, Mazet N (2003) Carbon 41:1715–1727
7. Dékány I, Haraszti T (1997) Colloid Surf A 123–124:391–401
8. Kotov NA, Haraszti T, Túri L, Zavala G, Geer RE, Dékány I, Fendler JH (1997) J Am Chem Soc 119:6821–6832
9. Haraszti T, Túri L, Dékány I, Fendler JH (1997) Model Chem 134:785–801
10. Decher G, Schlenhoff JB (2003) Multilayer Thin Films (Sequential Assembly of Nanocomposite Materials). Wiley-VCH, Weinheim
11. Lewis B, Anderson JC (1978) Nucleation and growth of thin films. Academic, New York
12. Decher G, Hong JD, Schmitt J (1992) Thin Solid Films 210:831–835
13. Lvov Y, Decher G, Möhwald H (1993) Langmuir 9:481–486
14. Decher G, Lvov Y, Schmitt J (1994) Thin Solid Films 244:772–777
15. Schmitt J, Grünewald T, Decher G, Kjaer K, Pershan PS, Lösche M (1993) Macromolecules 26:7058–7063
16. Sukhorukov GB, Möhwald H, Decher G, Lvov YM (1996) Thin Solid Films 284–285:220–223
17. Zang J, Wang Zhong-lin, Liu J, Chen S, Liu Ghang-yu (2003) Self-Assembled Nanostructures. Kluwer/Plenum
18. Crepaldi EL, Valim JB (1998) Quim Nova 21:300–311
19. You Y, Zhao H, Vance GF (2002) Colloid Surf A 205:161–172
20. Prinetto F, Ghiotti G, Graffin P, Tichit D (2000) Micropor Mesopor Mater 39:229–247
20. Unnikrishnan R, Narayanan S (1999) J Mol Catal A 144:173–179
22. Malherbe F, Depège C, Forano C, Besse JP, Atkins MP, Sharma B, Wade SR (1998) Appl Clay Sci 13:451–466
23. Rives V (2002) Appl Clay Sci 22:75–76
24. Kam S-K, Gregory J (1999) Colloid Surf A 159:165–179
25. Schwarz S, Eichhorn K-J, Wischerhoff E, Laschewsky A (1999) Colloid Surf A 159:491–501